THE RENDERING OF BUILDING TEXTURE FROM LAND-BASED VIDEO

Zuxun Zhang, Zhizhong Kang
School of Remote Sensing and Information Engineering, Wuhan Univ., Wuhan 430079, P.R. China - (zxzhang , zzkang)@supresoft.com.cn

KEY WORDS: Rendering, Mobile Mapping; Image Sequences; Texture; Mosaic; Rectification; Distortion

ABSTRACT:

Mobile mapping is a hot issue in the communities of photogrammetry and computer vision nowadays. Mobile mapping systems represent a significant advance in integrated, multi-sensor digital mapping technology, providing an innovative path towards rapid and cost-effective collection of high-quality and up-to-date spatial information. Therefore how to acquire geometric and texture information from the images for reducing human operations and enhancing efficiency is a challenge in mobile mapping data processing. In this paper, the rendering of building texture from land-based video is implemented. Firstly, some preprocessing of images is implemented. The occlusion of tree is removed because it goes against the extraction of lines from buildings. Close-ranged DC images are greatly affected by lens distortion, so lens distortion is calibrated and the influence is eliminated accordingly. Then, Land-based Video image sequences are automatically rectified to eliminate nonlinear distortion thanks to the large obliquity of the posture of DC. The building texture is finally mosaic from rectified image sequence and refined by the process of texture analysis.

1. INTRODUCTION

Real texture data, i.e. images, are required to make building objects more genuine in 3D city modeling(3DCM). Textures of terrains and the top of buildings are acquired from aerial images presently. The textures of building facades, however, are still acquired from images taken manually with digital camera. Since lacking index of images, the processes of searching images, preprocessing images and corresponding images with buildings are implemented manually. As a result, the problems of low efficiency and high labour intensity emerge. Therefore, it's becoming a hot issue in communities of digital photogrammetry , GIS and computer vision that how to solve these problems and relevant research are carried out (Debevec.P et al., 1996 ; Cipolla.R et al., 1999).

The acquisition of land-based video for buildings has the characteristics of convenience and rapidness. The resolution of textures obtained from land-based video is furthermore higher than those obtained from helicopter-based video. Therefore, it will be aided greatly by the automatic processing of textures from land-based video that the rapid reconstruction of texture for building facades in 3DCM. Accordingly, it's discussed in this article that the rendering of building textures from land-based video.

Firstly two groups lines are extracted from a single image. The occlusion of tree is removed employed the information of hue and lines with regular orientation because it goes against the extraction of lines from buildings. Close-ranged DC images have nonlinear distortion due to the large obliquity of the posture of DC and obvious lens distortion. Radial lens distortion parameter $k1$ is estimated because the major part of the lens distortion is eliminated by applying it only. Due to lens distortion, straight lines in object space appear as slightly curved lines in the image. Here we break up long curved image lines into smaller sections extracted later. Therefore, those sections extracted along the same curved image line are bound to be collinear. A model of adjustment system is then evolved according to this conclusion to estimate the radial lens distortion parameter $k1$.To eliminate the nonlinear distortion cause by large obliquity of the posture of DC, the automatic rectification of images is implemented. The key of automatic rectification of images is how to acquire camera parameters from the image information. Since the shape of buildings is always regular, there are many straight lines in building facades parallel to X-axis and Y-axis in object space. Namely the orientation of these lines is known. Therefore, it is presented to calibrate DC parameters that an algorithm combined with the constraint of straight lines bundle and the constraint of known orientation of parallel lines in object space.

The automatically mosaic process of façade texture is finally implemented employed the strategy of selecting mosaic point pair combined with correlation coefficient and geometric constraint of relative orientation. Tone adjustment is completed for the color difference between each two images contributing to illumination.

2. ESTIMATION OF LENS DISTORTION

As we know, close-ranged DC images are greatly affected by lens distortion and the influence should be eliminated accordingly. In this article, an algorithm that estimates lens distortion according to the curvature of straight lines thanks to lens distortion. Because the major part of the lens distortion is

a. A straight line extracted

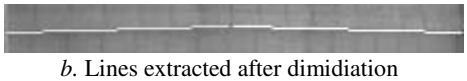

b. Lines extracted after dimidiation

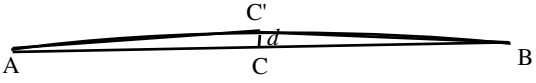

c. The curvature of straight lines

Fig.1 The determination of curvature of straight lines caused by lens distortion

eliminated by applying parameter k_1, only parameter k_1 is estimated in the article.

As Fig.1a illustrated, a straight line is extracted in the image while the actual line is slightly curved due to lens distortion. Therefore the line extracted is dimidiated and each line section is extracted again. The extracted result is illustrated as Fig.1b. The two lines extracted cannot obviously satisfy the condition of collinearity thanks to lens distortion. As Fig.1c illustrated, *d* denotes the displacement of point *C* to point *C*□caused by lens distortion. Therefore, *d* can be employed to calibrate the lens distortion. A model of least adjustment is then evolved according to this conclusion to estimate the radial lens distortion parameter *k*1.

3. OCCLUSION REMOVAL

Since the occlusion of trees goes against the extraction of lines from buildings, the occlusion area should be automatically distinguished and removed.

3.1 Occlusion Removal Employed Hue Information

As Fig. 2a illustrated, it is taken for granted that color information can be employed to remove the occlusion of trees because of the color similarity of trees. Therefore, a '80~200' range of hue value is chosen to determine whether a pixel lies in the occlusion area. The result of occlusion removal is illustrated in Fig.2b. As we can see, some pixels in the red ellipse area which hue values are out of the range we chosen are remained although they are lying in the occlusion area, meanwhile some pixels in the green ellipse area vice versa. A conclusion is drawn, thereupon, that the result of occlusion removal only employed hue information comes out lacking stability.

Here it is presented to improve the stability that an algorithm of Occlusion removal employed information of hue and lines.

3.2 Occlusion Removal Employed Information of Hue and Lines

Lines are Firstly extracted in the original image as Fig. 2a illustrated. As we can see, lines on the building façade are almost corresponding to object lines parallel to *X*-axis and *Y*-axis in the object space, therefore their orientation are regular while lines in the trees vice versa. The information of lines with regular orientation, thereupon, can be used to detect the occlusion area combined with hue information. The process is presented below:

a. Lines extracted

b. Occlusion removal employed hue information

c. Occlusion removal employed information of hue and lines

Fig.2 Occlusion removal

1) Divide the original image into 40×40 rectangular grids with grid size of 18 pixels×12 pixels.
2) Count the number of pixels which hue values are in the range of 80~200 in every grid. If the number is 80% of total, this grid is deemed to lie in occlusion area and removed. Otherwise, the grid will be quartered and the same operation will impose on new grids.
3) The density of lines with regular orientation in the whole image is determined by Eqs.1

$$\rho_l = \frac{\sum_{i=1}^{n} Li}{S} \qquad (1)$$

With,

ρ_l : The density of lines with regular orientation in the whole image;

Li : The length of line *i*(pixel);

S: The area of the whole image(pixel^2).

4) Calculate the densities of lines with regular orientation respectively in grids having not been removed. If the density of a grid is smaller than that of whole image, this grid is deemed to lie in occlusion area and removed.

The result of occlusion removal, as illustrated in Fig.2c, is obviously better than that illustrated in Fig.2b.

4. THE AUTOMATIC RECTIFICATION OF FACADE TEXTURE

Since building facades are planar, there are two groups of lines parallel to *X*-axis and *Y*-axis in object space respectively on each of them. As a result, only focus *f* and three angular orientation parameters φ , ω , k can be calculated according to theories of vanishing point geometry. Therefore façade textures are rectified employed *f* and φ , ω , k with principle point fixed at the center of image. The process of rectification is

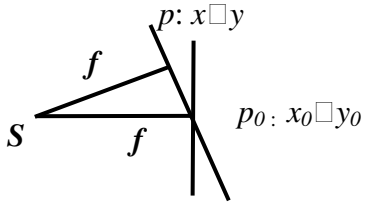

Fig. 3 The process of rectification

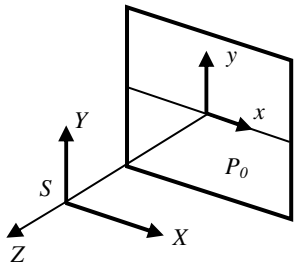

Fig. 4 the relationship between p_0 and object space coordinate system

illustrated as Fig.3. For close-ranged DC images, the coordinate system of object space is set up as Fig.4 illustrated. The façade textures are rectified onto plumb plane accordingly.

4.1 The Determination of Vanishing Point and Initial Values of DC Angular Parameters.

Vanishing point $V(x_V, y_V)$ is the intersection point of a set of straight lines which are parallel in object space. It means that each straight line such as line *ij* belong to this set must be passed through the vanishing point as shown in Fig.5. So Eqs.2 is evolved.

$$d = (y_j - y_i)\frac{(x_V - x_i)}{s_{iV}} - (x_j - x_i)\frac{(y_V - y_i)}{s_{iV}} \tag{2}$$

where, d is the distance of point j to line iV.

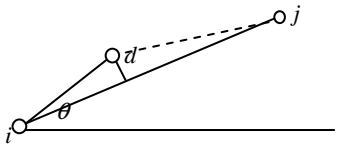

Fig. 5 The constrain of Straight lines bundle

From Eqs.2 a model of adjustment system of observations and parameters is deduced to determine vanishing point. Then initial values of DC angular parameters are decomposed according to vanishing point geometry (B. Caprile. et al., 1990).

4.2 The Calibration of DC Angular Parameters

Two algorithms of calibration of DC angular parameters are presented here.

4.2.1 The Calibration Employed the Constraint of Straight Lines Bundle: According to vanishing point geometry vanishing point coordinate (x_V , y_V) in Eqs.2 is replaced with interior and exterior orientation (angular) parameters. Then a model of adjustment system of observations and parameters employed the constraint of straight lines bundle is deduced to calibrate DC angular parameters while interior orientation parameters are fixed in the adjustment system. Because the initial value of orientation parameters is decomposed from vanishing point coordinates, the accuracy is not always high owing to the quality of images and the error of line extraction. Therefore, It has a small convergent radius that the model of adjustment system employed the constraint of straight lines bundle. As a result, the model of adjustment system is not robust.

In this article, it's introduced to control the adjustment system that the constraint of known orientation of parallel lines in object space.

4.2.2 The Model of Adjustment System Controlled by the Constraint of Known Orientation of Parallel Lines in Object Space: There are two group lines parallel to *X*-axis and *Y*-axis in object space respectively. Their projections in image space are involved in the adjustment system, consequently the projections of these two group lines in rectified image should be parallel to *X*-axis and *Y*-axis in object space respectively in ideal instance (As illustrated in Fig.3 and Fig.4). Namely Eqs.3 and 4 are deduced.

In *X* direction:

$$-f\frac{b_1x_i + b_2y_i - b_3f}{c_1x_i + c_2y_i - c_3f} = -f\frac{b_1x_j + b_2y_j - b_3f}{c_1x_j + c_2y_j - c_3f} \tag{3}$$

In *Y* direction:

$$-f\frac{a_1x_m + a_2y_m - a_3f}{c_1x_m + c_2y_m - c_3f} = -f\frac{a_1x_n + a_2y_n - a_3f}{c_1x_n + c_2y_n - c_3f} \tag{4}$$

With:

(x_i □ y_i),(x_j □ y_j): the coordinates of two end points of line parallel to *X*-axis

(x_m □ y_m),(x_n □ y_n): the coordinates of two end points of line parallel to *Y*-axis

f : focal length

$\begin{bmatrix} a_1 & a_2 & a_3 \\ b_1 & b_2 & b_3 \\ c_1 & c_2 & c_3 \end{bmatrix}$: rotation matrix

Eqs.3 and 4 can be control condition for the calibration of DC angular parameters. Therefore it's deduced that a model of adjustment system combined with constraints of straight lines bundle and known orientation of parallel lines in object space. As the experimental results showing, the model of adjustment system deduced here has the characteristics of large convergent radius and high stability.

5. THE AUTOMATIC MOSAIC OF FACADE TEXTURE

Usually for big buildings, façade texture is covered by several images instead of only one image. Therefore to acquire the whole façade texture, mosaic process is required. Since façade textures are all rectified onto plumb plane, only the displacements d_x, d_y in *X*-axis and *Y*-axis respectively are needed to determine in mosaic process. Thereupon, the question is how to determine the displacements d_x, d_y.

Fig.6 Corresponding points matched

Firstly, corresponding points are automatically matched between each two adjacent images. As Fig.6 illustrated, there are 295 corresponding point pairs acquired. Because of the similarity of texture, some false point pairs are also obtained. Therefore, an optimal point pair should be picked out as mosaic point pair by which the displacements d_x, d_y are determined. The strategy of selecting mosaic point pair is then presented.

5.1 Selecting Mosaic Point Pair by Maximum Correlation Coefficient

As we know, correlation coefficient is employed to determine whether the point pair of interest is corresponding. The larger the correlation coefficient is, the more likely it is that the point pair of interest is corresponding. Consequently it's taken for granted that the point pair with maximum correlation coefficient should be mosaic point pair. The displacements d_x, d_y are calculated by the mosaic point pair and façade textures are mosaic as Fig.7 illustrated. The result is not satisfying because even the point pair with maximum correlation coefficient is not really corresponding thanks to the similarity of texture.

Fig.7 The mosaic result employed the strategy of maximum correlation coefficient

Hence to acquire a real corresponding point pair, geometric constraint needs to be introduced.

5.2 Selecting Mosaic Point Pair Combined with Correlation Coefficient and Geometric Constraint

Relative orientation process is implemented employed the corresponding point pairs matched above and the vertical parallax Q of every corresponding point pair is acquired meanwhile. Therefore the corresponding factor is calculated as below.

$$F_i = \frac{Q_i}{1+\rho_i} \tag{5}$$

with:

F_i : the corresponding factor of point pair i, the larger $\frac{1}{F_i}$ is, the more likely it is that point pair i is corresponding

Q_i : the vertical parallax of point pair i

ρ_i : the correlation coefficient of point pair i, the value of ρ_i is 100 when point pair i is fully correlated

Fig.8 The mosaic result employed the strategy combined with correlation coefficient and geometric constraint

According to the corresponding factor, the mosaic point pair is obtained and façade textures are mosaic as Fig.8 illustrated. The result is obviously satisfying.

5.3 Tone Adjustment

Because of the illumination, the color difference exists between each two images. In this paper, it is presented that an algorithm of tone adjustment by maximum intensity difference detected to eliminate the color difference.

Firstly, the intersectional area is determined according to the corresponding points matched. The maximum intensity difference is then detected in this area and the tone of the right image is adjusted by linear mapping according to it.

6. EXPERIMENTAL RESULTS

Façade textures are acquired from image sequence extracted from video obtained by DV. The size of image is 720 pixels× 480 pixels.

6.1 The Comparison between Two Kinds of Least Square Adjustment Models

To compare the difference of convergent radius and stability between the model employed the constraint of straight lines bundle (Model A) and the model controlled by the constraint of known orientation of parallel lines in object space (Model B),

(a) Model B (b) Model A

Fig.9 Rectified Images (Histogram of Angle)

(a) Model B (b) Model A

Fig. 10 Rectified Images (Histogram of Angle with the Geometric Constrain of Normal Vector to Interpretation plane)

(a) Model B (b) Model A

Fig. 11 Rectified Images (Histogram of Angle with the Geometric Constrain of Normal Vector to Interpretation plane)

the least square adjustments employed these two model are implemented based on the results of grouping lines by three methods, i.e. grouping lines by angle histogram, by angle histogram with geometric constraint of normal vector to interpretation plane and by initial value acquired artificially. The results of rectification are illustrated as Fig.9~11.

The distributing of vanishing point coordinates, angular parameters and focus is shown in Fig.12 based on the results of least square adjustment above (The hollow denotes model A while the solid denotes model B).

From the distributing above, a conclusion is easily drawn that model B has larger convergent radius and higher stability than those of model A. Namely, the values acquired by model B are generally optimal while those acquired by model A are locally optimal.

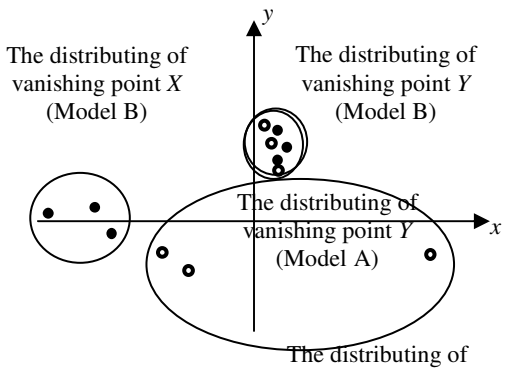

(a) The distributing of vanishing point

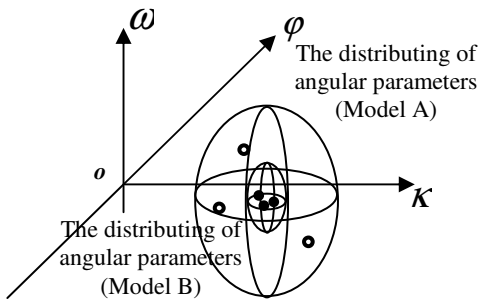

(b) The distributing of angular parameters

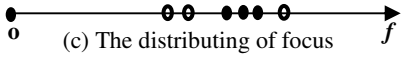

(c) The distributing of focus

Fig. 12 Convergence Distributing

6.2 The Elimination of Lens Distortion

There are 408 lines extracted in the image as Fig.13a illustrated. And then 68 lines which lengths are over 60 pixels are dimidiated and extracted again. The result is shown in Fig.13b. The lens distortion is estimated used those lines extracted after dimidiation and the result of correction of lens distortion is illustrated in Fig.13c. As we can see, The lines curving thanks to lens distortion obviously became straight after lens distortion correction. That is the lens distortion was eliminated.

*a.*Lines extracted *b.* Lines extracted after dimidiatiaon *c.* Result of lens distortion correction

Fig13. Lens distortion correction

6.3 The Mosaic of Façade Texture

Fig.14 is the comparison of mosaic results of façade texture employed two strategy presented above. The mosaic result used the strategy of selecting mosaic point pair combined with correlation coefficient and geometric constraint is obviously much better than that employed the strategy of selecting mosaic point pair by maximum correlation coefficient.

After the processes of tone adjustment and texture analysis, more refined façade texture is acquired as Fig.15 illustrated.

7. CONCLUSIONS

The algorithm of rendering of building façade texture from land-based image sequence has been presented. Some experiments has been conducted with land-based image sequence acquired by DV. The result is satisfying and several

a. maximum correlation coefficient

b. combined with correlation coefficient and geometric constraint

Fig.14 the comparison of mosaic results of façade texture

conclusions are drawn as below.

- The curvature of straight lines caused by lens distortion can be detected used those lines extracted after the dimidiation of every long straight line. Therefore the lens distortion can be estimated according to the curvature detected. The method to estimate lens distortion presented in this article is proven to be straightforward and effective by the experiments carried out.
- it is taken for granted that color information can be employed to remove the occlusion of trees because of the

Fig. 15 Refined Texture for Building Facade

color similarity of trees. However the result of occlusion

removal only employed hue information comes out lacking stability. As we can see, lines on the building façade are almost corresponding to object lines parallel to *X*-axis and *Y*-axis in the object space, therefore their orientation are regular while those in the trees vice versa. The information of lines with regular orientation, thereupon, can be used to detect the occlusion area combined with hue information. It's proven that more stable result of occlusion removal can be acquired employed this method.

- Since it has a small convergent radius that the model of least square adjustment employed the constraint of straight lines bundle, the model is sensitive to initial value which tends to be affected by the quality of image and the errors of line extraction. However, it has a larger convergent radius and higher stability that the model of adjustment system controlled by the constraint of known orientation of parallel lines in object space presented in this article, thanks to the strictly geometric constraint to control the calibration of DC parameters.

- Two strategies of selecting mosaic point pair are compared in this article. It has been proven by experiments that the strategy combined with correlation coefficient and geometric constraint of relative orientation is better than that taking only correlation coefficient into consider.

REFERENCES

B. Caprile and V. Torre, 1990. Using Vanishing Points for Camera Calibration, *IJCV*, 4(2), pp. 127–140.

Cipolla.R. Robertson. D.P and Boyer.E.G. Photobuilder, (June) 1999. 3D models of architectural scenes from uncalibrated images. Proc. IEEE International Conference on Multimedia Computing and Systems, Firenze, volume I, pp.25-31.

Debevec.P Taylor.C.J Malik.J., 1996. Modeling and Rendering Architecture from Photographs: A Hybrid Geometry- and Image-Based Approach, Proc. Of SIGGRAPH 96.

ACKNOWLEDGMENTS

We wish to thank the project of Natural Scientific Foundation of China titled "Three-Dimensional City Model Generation by Videogrammetry" with the serial number 40301041 for its support to our research.